Generalized Bethe approximation

Douglas Poland
Department of Chemistry, The Johns Hopkins University, Baltimore, Maryland 21218
(Received 15 June 1998; revised manuscript received 22 October 1998)

We generalize the Bethe approximation by writing the activity of the system of interest relative to the activity of the same system in the high-temperature limit (assumed known) times a function involving the grand partition function for a small block of the system. The high-temperature limit of the system can involve extended excluded volume effects that give rise to order-disorder phase transitions. The generalized Bethe approximation can be viewed as an approximate method for adding the effect of attractions to a hard-particle system. As an example we treat the lattice gas on the plane-square lattice with nearest-neighbor exclusion and next-nearest neighbor attraction. The properties of the infinite-temperature limit (nearest-neighbor exclusion only) are obtained using Padé approximants to low- and high-density series. The Bethe approximation then adds in the effect of attractions and gives a phase diagram similar to that obtained from exact series.
[S1063-651X(99)09802-5]

PACS number(s): 05.20.−y, 05.50.+q, 05.70.Fh, 05.70.Jk

I. INTRODUCTION

The Bethe approximation is a combinatorial approach to cooperative systems (lattice models for fluids, magnets, alloys, etc.) in which phase transitions and critical phenomena are found, the results generally being better than those found in mean-field theory for the same system. It was first introduced as an approximate method to treat the statistical mechanics of alloys by Bethe [1] and then, in a different manner, by Guggenheim who showed that the two approaches were identical [2]. It is sometimes referred to as the Bethe-Guggenheim approximation or as the quasichemical approximation. It is described clearly in the books by Hill [3,4]. An important property of the Bethe approximation is that it is the exact solution [5] for the properties of a nontrivial system, namely, for ever-branching lattices, as illustrated in Fig. 1 for the cases of three- and two-coordinate branching (the latter case being the one-dimensional lattice). Since the one-dimensional lattice is a Bethe lattice, the Bethe approximation is exact for the nearest-neighbor one-dimensional Ising model [6,7].

In the present paper we show that the Bethe approximation is equivalent to the following simple procedure. We take a small block of the lattice (in the simplest form this is just two contiguous lattice sites or a bond) and write the grand partition function for the block using a special activity ζ that takes into account the sharing of particles between neighboring blocks. Then if z is the activity of the system of interest, this activity is given in the Bethe approximation by the following expression:

$$\frac{z(\rho,T)}{z(\rho,\infty)}=\frac{\zeta(\rho,T)}{\zeta(\rho,\infty)} \tag{1.1}$$

or

$$z(\rho,T)=z(\rho,\infty)\frac{\zeta(\rho,T)}{\zeta(\rho,\infty)}. \tag{1.2}$$

First we note that all of the activities correspond to the same net density ρ. The quantity $\zeta(\rho,T)$ is the activity of the block at a general temperature T while $\zeta(\rho,\infty)$ is the activity of the block at the same density ρ but at an infinite temperature (washing out all attractive interactions). The quantity $z(\rho,T)$ is the approximate activity of the system of interest at density ρ and general temperature T while $z(\rho,\infty)$ is the activity of the system at the same density but at infinite temperature; the method requires that we are able to calculate the high-temperature limit of the activity of the system of interest.

The important feature of Eq. (1.2) is that the reference system (high-temperature limit) can be a hard-particle lattice gas that exhibits a gas-solid phase transition. The Bethe approximation then adds in the perturbations due to attractions that can introduce additional or altered phase transitions in the system. It is thus a useful tool with which to investigate multiple phase transitions in lattice gases.

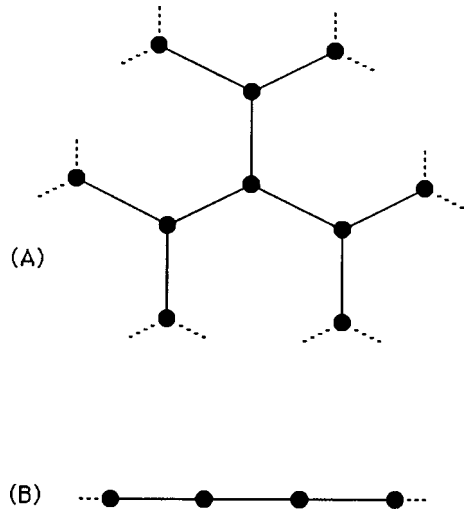

FIG. 1. Illustration of Bethe (ever-branching) lattices. At each junction there are c branches with no return loops. (a) The case of $c=3$. (b) The case of $c=2$, which is equivalent to the one-dimensional lattice. The Bethe approximation is exact on such lattices.

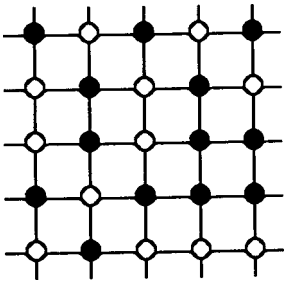

FIG. 2. Illustration of the Ising model on the plane-square lattice. Each lattice site can be occupied by a particle (solid circle) or not (open circle). At most one particle can occupy a lattice site and particles on nearest-neighbor lattice sites experience an attractive energy of interaction.

We will derive Eq. (1.1) in the next section. In the Appendix we will show that Eq. (1.1) is a characteristic property of a branching Markov chain. Since the ever-branching lattice, as illustrated in Fig. 1, can be treated exactly as a branching Markov chain, Eq. (1.1) implies that the Bethe approximation is exact for such systems. The advantage of this generalized approach to the Bethe approximation is that all we need is the grand partition function for the block of lattice sites and the high-temperature limit of the system of interest. Once we have Eq. (1.1) there are no combinatorics required. In Sec. III we illustrate the method for the Ising model while in Sec. IV we apply the method to the lattice gas on the plane-square lattice with nearest-neighbor exclusion and next-nearest-neighbor attraction. In the following paper [8] we use the generalized Bethe approximation to treat a lattice gas model that exhibits gas, liquid, and solid phases. The qualitative behavior of the phase diagrams found in the Bethe approximation for this system are corroborated by results from exact series.

II. RATIO FORMULA

In this section we derive the ratio formula of Eq. (1.1). We begin by using the example of the standard Ising model for a lattice gas on the plane-square lattice as illustrated in Fig. 2. A site can be occupied or unoccupied by a particle (at most one particle per site), a feature illustrated in Fig. 2, respectively, by solid and open circles. Particles on neighboring lattice sites experience an attractive energy of interaction. We take M as the number of lattice sites, N as the number of particles, and $x=\exp[-\varepsilon/kT]$ as the Boltzmann factor between nearest-neighbor occupied sites (where ϵ is the negative, or attractive, nearest-neighbor interaction energy). Then the standard presentation [3,4] of the Bethe approximation writes the canonical partition function as follows:

$$Q(M,N,T)=C(M,N)Q'(M,N,T), \tag{2.1}$$

where Q' is the partition function for independent blocks and $C(M,N)$ is a correction factor that gives the correct value of Q in the high-temperature limit ($T\to\infty$ or $x\to 1$),

$$C(M,N)=Q(M,N,\infty)/Q'(M,N,\infty). \tag{2.2}$$

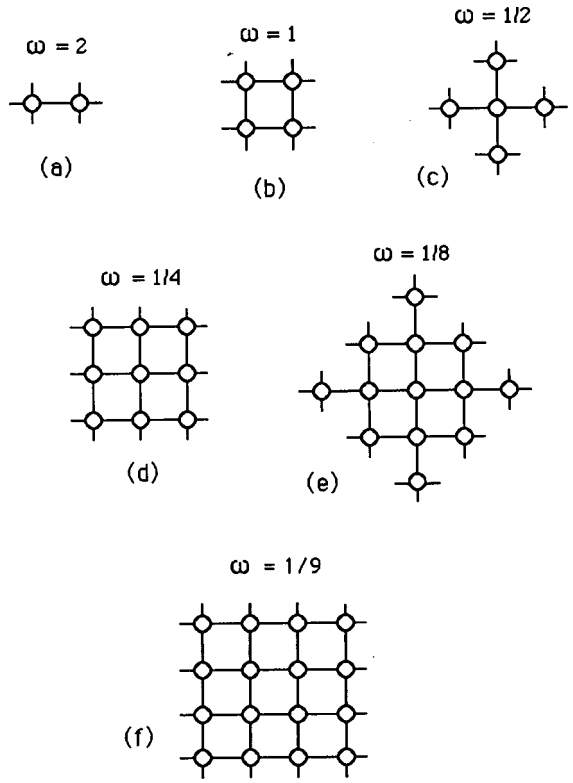

FIG. 3. Illustration of blocks of lattice sites of various sizes on the plane-square lattice. The ω's are geometric factors defined in Eq. (2.3) that relate the maximum number of such blocks to the number of lattice sites.

This of course requires that one know the high-temperature limit $Q(M,N,\infty)$.

The blocks can be of any size and shape as long as one can cover all of the lattice sites in a regular manner. Several different blocks for the two-dimensional square lattice are illustrated in Fig. 3. The blocks are placed on the lattice so that the sites on the border of one block overlap with those of the neighboring block. This feature is illustrated in Fig. 4(a), where we show the neighboring placement of two blocks of type (d) from Fig. 3. The same configuration is shown in Fig. 4(b), where we pull the blocks apart a small amount for clarity. The fact that some particles and bonds are shared between two blocks will be taken into account in the con-

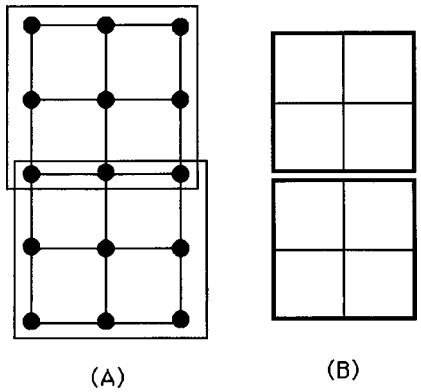

FIG. 4. Illustrating of the overlapping of neighboring blocks. (a) Two neighboring blocks of type (d) from Fig. 3. (b) Simpler view of the same block configuration.

struction of the block grand partition function. A feature we will not address here is the case where there are bonds that cross the boundary between two neighboring blocks. This type of interaction can be treated using a mean-field approximation, but none of the models we will treat here and in the following paper [8] require this feature.

The maximum number of blocks that can be placed on a lattice is given by the relation

$$N_{\max}=\omega M. \tag{2.3}$$

The coefficient ω is indicated for the various blocks shown in Fig. 3; ω is usually less than 1 for large blocks but is 2 for bonds [case (a) in Fig. 3] on the plane-square lattice. The original form of the Bethe approximation was given for the simplest type of block, namely a pair of neighboring lattice sites. It was soon extended to larger blocks of lattice sites [9–11].

To construct Q' for a given type of block one first constructs the canonical partition functions $q_i(x)$ for the different possible particle configurations in a block; if there are n lattice sites in a block the index i will run over 2^n different states. The q_i are simply products of x factors reflecting the number of bonds in a particular cluster. If a bond is in the interior of a cluster it contributes a full x factor to q_i while if it is on the edge of a cluster, so that it is shared with another cluster, it contributes a factor $\sqrt{x}$ to q_i. Taking N_i as the number of blocks of type I, Q' is then given by summing over all numbers and random arrangements of the blocks on the lattice,

$$Q'(M,N,T)=\sum_{\{N_i\}}\frac{(\Sigma_i N_i)!}{\Pi_i N_i!}\prod_i q_i{}^{N_i}=\sum_{\{N_i\}} t\{N_i\}, \tag{2.4}$$

where the $t\{N_i\}$ are defined by Eq. (2.4). The sums over the N_i are subject to the following two constraints:

$$\sum_i N_i=\omega M \quad \text{(conservation of blocks)}, \tag{2.5}$$

$$\sum_i \nu_i N_i=N \quad \text{(conservation of particles)}, \tag{2.6}$$

where ν_i is the number of particles in configuration i that can be assigned solely to that block [if a particle is on border site in a block, it must be counted as shared by more than one block in the tally for the density in Eq. (2.6)]. We find the most probable set of the N_i subject to the above two constraints by using the standard Lagrange-undetermined-multiplier method. We construct the following expression:

$$\frac{\partial \ln t}{\partial N_i}+\ln a\,\frac{\partial \Sigma_j N_j}{\partial N_i}+\ln \zeta\,\frac{\partial \Sigma_j \nu_j N_j}{\partial N_i}=0, \tag{2.7}$$

where a and ζ are the undetermined multipliers whose value is unknown at this stage. Using Stirling's approximation for the factorials in Eq. (2.4) and taking the required derivatives in Eq. (2.7) gives the most probable value of the general N_i (which we designate as N_i^*),

$$\frac{N_i^*}{\Sigma_i N_i^*}=P_i=a\,\zeta^{\nu_i}q_i. \tag{2.8}$$

The quantity given in Eq. (2.8) is simply the fraction, or probability, of blocks of type i. The a multiplier is easily eliminated by requiring that the sum over the P_i is one

$$a=1\Big/\sum_i \zeta^{\nu_i}q_i \tag{2.9}$$

or

$$P_i=\zeta^{\nu_i}q_i\Big/\sum_j \zeta^{\nu_j}q_j. \tag{2.10}$$

The form of Eq. (2.10) suggests that we define a block grand partition function, interpreting the undetermined multiplier ζ as a kind of activity,

$$\xi=\sum_i \zeta^{\nu_i}q_i. \tag{2.11}$$

Then the probability of a block type is obtained in the standard fashion,

$$P_i=\frac{\partial \ln \xi}{\partial \ln q_i}. \tag{2.12}$$

Formally the quantity ζ can be determined by taking the ratio of the constraint equations

$$\frac{\Sigma_i \nu_i N_i^*}{\Sigma_i N_i^*}=\frac{N}{\omega M}=\frac{\rho}{\omega} \tag{2.13}$$

or

$$\rho=\omega\frac{\partial \ln \xi}{\partial \ln \zeta}, \tag{2.14}$$

where

$$\rho=N/M \tag{2.15}$$

and ω is the geometric factor defined in Eq. (2.3).

We now return to Eq. (2.1) and calculate the chemical potential in the standard way,

$$\beta\mu(T)=-\frac{\partial \ln Q}{\partial N}=-\frac{\partial \ln C}{\partial N}-\frac{\partial \ln Q'}{\partial N}. \tag{2.16}$$

Now

$$\beta\mu'(T)=-\frac{\partial \ln Q'}{\partial N}. \tag{2.17}$$

Using Eq. (2.2) we have

$$-\frac{\partial \ln C}{\partial N}=\beta\mu(\infty)-\beta\mu'(\infty), \tag{2.18}$$

which are the high-temperature limits of the two activities. Combining (2.16)–(2.18) we have

$$\beta\mu(T)-\beta\mu'(T)=\beta\mu(\infty)-\beta\mu'(\infty). \tag{2.19}$$

The relation between the activity and the chemical potential is

$$z=\exp[\beta\mu-\beta\mu^0], \tag{2.20}$$

where $\beta\mu^0$ is the standard part of the chemical potential (for lattice gases this is the momentum contribution).

The grand partition function for the total system in the block approximation can be written as

$$\Xi'=\xi(x,\zeta)^{\omega M}=1+\cdots+(\zeta x^2)^M, \tag{2.21}$$

which illustrates that ζ is the activity in the prime system. Thus we have

$$\beta\mu'=-\frac{\partial \ln Q'}{\partial N}=\ln\zeta. \tag{2.22}$$

Thus using Eqs. (2.20) and (2.22) in Eq. (2.19) gives the ratio formula of Eq. (1.1).

We can obtain an equation similar to Eq. (2.19) involving the pressures. We start with Eq. (2.1) and instead of taking the derivative with respect to N to give the chemical potential we take the derivative with respect to M (the analog of the volume V for the discrete system) obtaining

$$\beta p(T)=\beta p(\infty)+[\beta p'(T)-\beta p'(\infty)], \tag{2.23}$$

where

$$\beta p'(T)=\omega\ln\xi(T) \quad \text{and} \quad \beta p'(\infty)=\omega\ln\xi(\infty). \tag{2.24}$$

The quantity $\beta p(1)$ is the high-temperature limit of the pressure for density ρ, a quantity we assume that we know.

III. ISING MODEL

As a specific example we continue to use the Ising model on the plane-square lattice. We treat the simplest type of block that contains the possibility of a nearest-neighbor interaction between particles, namely, the pair of sites illustrated in Fig. 3(a). Using 0's and 1's to indicate empty and occupied lattice sites, respectively, there are four possible states for a pair of contiguous lattice sites: 00, 01, 10, and 11. The quantity ξ is then a sum over these four states. In using ξ of Eq. (2.11) we require the exponents v_i that tell how the particles in a particular configuration are shared between pairs of sites. It is convenient to factor the quantity ζ^{v_i} into contributions from factors per site of the form ζ^α with a characteristic value of α for each different kind of lattice site in the block. For the block we are considering an empty site gets a factor $\zeta^0=1(\alpha=0)$ while each occupied sites gets a factor $\zeta^{1/4}$ $(\alpha=\frac{1}{4})$; the $\frac{1}{4}$ arises since, for a lattice with coordination number $c=4$, each occupied site is shared by four different bonds). The ξ for this model is then

$$\xi=1+2\zeta^{1/4}+x\zeta^{1/2}. \tag{3.1}$$

And this is all there is to constructing the Bethe approximation for the Ising model on the plane-square lattice (no combinatorics!).

We then proceed by picking any set of values of ζ and x we want and calculating the density from Eq. (3.1),

$$\rho=\omega\frac{\partial\ln\xi}{\partial\ln\zeta}=\frac{\zeta^{1/4}+x\zeta^{1/2}}{1+2\zeta^{1/4}+x\zeta^{1/2}}. \tag{3.2}$$

Given the above value of ρ we then calculate the value of $\zeta(1)$, taking $x=1$, required to give this same density, namely

$$\zeta(1)=\left(\frac{\rho}{1-\rho}\right)^4. \tag{3.3}$$

Next we require the exact value of the activity in the system of interest that also corresponds to the density ρ. At $x=1$ the overall exact grand partition function is

$$\Xi=(1+z)^M=e^{pM/kT}, \tag{3.4}$$

giving

$$p/kT=\ln(1+z)=-\ln(1-\rho) \tag{3.5}$$

and

$$\rho=\frac{z}{1+z} \tag{3.6}$$

or

$$z(1)=\frac{\rho}{1-\rho}. \tag{3.7}$$

Combining Eqs. (3.3) and (3.7), and the initial value of $\zeta(x)$, we then have

$$z(x)=\zeta(x)\left(\frac{z(1)}{\zeta(1)}\right)=\zeta(x)\left(\frac{1-\rho}{\rho}\right)^3. \tag{3.8}$$

The pressure is given by

$$\beta p(x)=-\ln(1-\rho)+\omega[\ln\xi(x)-\ln\xi(1)]. \tag{3.9}$$

Equations (3.8) and (3.9) give precisely the same results as the conventional Bethe approximation [3,4].

For the nearest-neighbor Ising model with general coordination number c Eq. (3.1) is

$$\xi=1+2\zeta^{1/c}+x\zeta^{2/c} \tag{3.10}$$

while Eq. (3.8) becomes

$$z(x)=\zeta(x)\left(\frac{1-\rho}{\rho}\right)^{C-1}. \tag{3.11}$$

The pressure equation (3.9) is the same with $\omega=c/2$. We note again that Eqs. (3.10) and (3.11) are all there is to the Bethe approximation for the Ising model on the level of pairs of sites. In the Appendix we show that Eq. (1.1) is a property of branching Markov chains so Eqs. (3.10) and (3.11) are the exact solution for ever-branching lattices as illustrated in Fig. 1.

The Bethe approximation for the Ising model is of interest since for $c>2$ it exhibits gas-liquid phase transitions and a critical point. For general c the critical value of x is

$$x_c = \left(\frac{c}{c-2} \right)^2, \tag{3.12}$$

which for the Ising model on the plane-square lattice gives $x_c = 4$ {which is to be compared [3,4] with the result from standard mean-field theory for the same model of $x_c = e = 2.718$ and the exact value of $x_c = [1/(\sqrt{2}-1)]^2 = 5.828$}. For $c = 2$ (the $1d$ Ising model) $x_c = 0$, which is equivalent to $T_c = 0$, i.e., the critical temperature is absolute zero).

The utility of an approximate method like the Bethe approximation is that for a very modest investment of effort, basically, Eq. (3.10), one obtains an approximate indication of the kind of phase transitions present in a system. The phase-transition behavior is best seen using the fugacity

$$y = z x^{c/2}, \tag{3.13}$$

which for $c = 4$ gives $y = z x^2$. The reason that this variable is of interest is that Lee and Yang proved [12] that the phase-transition singularities in any nearest-neighbor Ising model occur when $y = 1$. In Fig. 5 we show the density as a function of fugacity for the Ising model on the plane-square lattice for $x = 3$, 4, and 5; since for this model $x_c = 4$ these values of x represent, respectively, the cases $x < x_c\ (T > T_c)$, $x = x_c\ (T = T_c)$, and $x > x_c\ (T < T_c)$. Above the critical temperature $\rho(y)$ exhibits a typical sigmoidal shape; at the critical temperature this function develops an inflection point at the midpoint; and, below the critical temperature the function develops the famous van der Waals loops. In Fig. 6 we show the pressure p/kT as a function of fugacity for the same cases shown in Fig. 5. Now the development of a first-order phase transition below the critical point is very clear: the $p(y)/kT$ curve develops a swallowtail kind of cusp. The swallowtail cusp itself is an artifact of the approximate method (the thermodynamic behavior in the cusp region is nonphysical), so one simply removes the cusp, leaving the crossing of branches of the $p(y)/kT$ curve representing the gas and liquid phases.

Lee and Yang [12] proved that a phase transition corresponds to a singularity in the grand partition function (or, equivalently, in the pressure). The kink in the $p(y)/kT$ curve left when the cusp is removed is the phase-transition singularity in the Bethe approximation. In Fig. 7 we interpret the case of $x = 5$ using parts of Figs. 5 and 6. Fig. 7(a) shows the pressure with the swallowtail cusp as given in Fig. 6. In Fig. 7(b) the cusp is removed, leaving the kink where the branches of the function crossed. To obtain the densities of the gas and liquid phases at the phase-transition point one takes the slope of p/kT on either side of the singularity point. Using L and H as symbols for the gas (L = low density) and liquid (H = high density) states one has

$$\rho_L = \left(\frac{\partial \beta p}{\partial \ln y} \right)_{y-} \quad \text{and} \quad \rho_H = \left(\frac{\partial \beta p}{\partial \ln y} \right)_{y+}, \tag{3.14}$$

where the subscripts $y-$ and $y+$ indicate that the slope is to be evaluated at $y = 1$ on the sides $y < 1$ and $y > 1$, respectively. The above slopes are schematically illustrated in Fig. 7(b) where the densities so obtained are then used in Fig. 7(c) to interpret the loops in the $\rho(y)$ curve as a jump discontinuity in the density at the first-order phase transition. Of course this procedure is equivalent to the Maxwell equal-area construction, but it is simpler to implement in that one can fit $p(y)/kT$ to a polynomial on either side of the kink and then calculate the crossing point (and the slopes at the crossing point) analytically. Knowing the gas and liquid densities at the phase transition as a function of temperature then gives the coexistence curve. One should note that the mean-field approximation shows the same qualitative behavior found in Figs. 5 and 6.

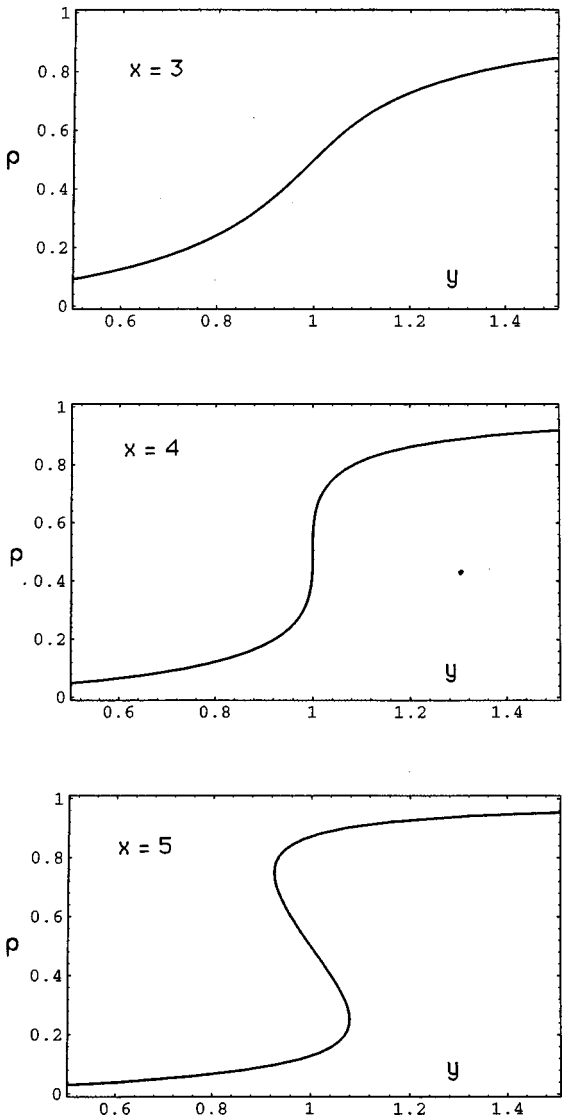

FIG. 5. The density as a function of fugacity [see Eq. (3.13)] for the Bethe approximation for the Ising model as given by Eq. (3.8) for three different temperatures ($x = 3$, $T > T_c$; $x = 4$, $T = T_c$; and $x = 5$, $T > T_c$).

Hill [3] has pointed out that the mean-field (or Bragg-Williams) approximation for the Ising model can be cast in the form of an average grand partition function per lattice site. Since this is not strictly a proper grand partition function, it is useful to point out the differences between that function and the block grand partition functions we are using. For the nearest-neighbor Ising model the mean-field canonical partition function for N particles on M sites with coordination number c is given by

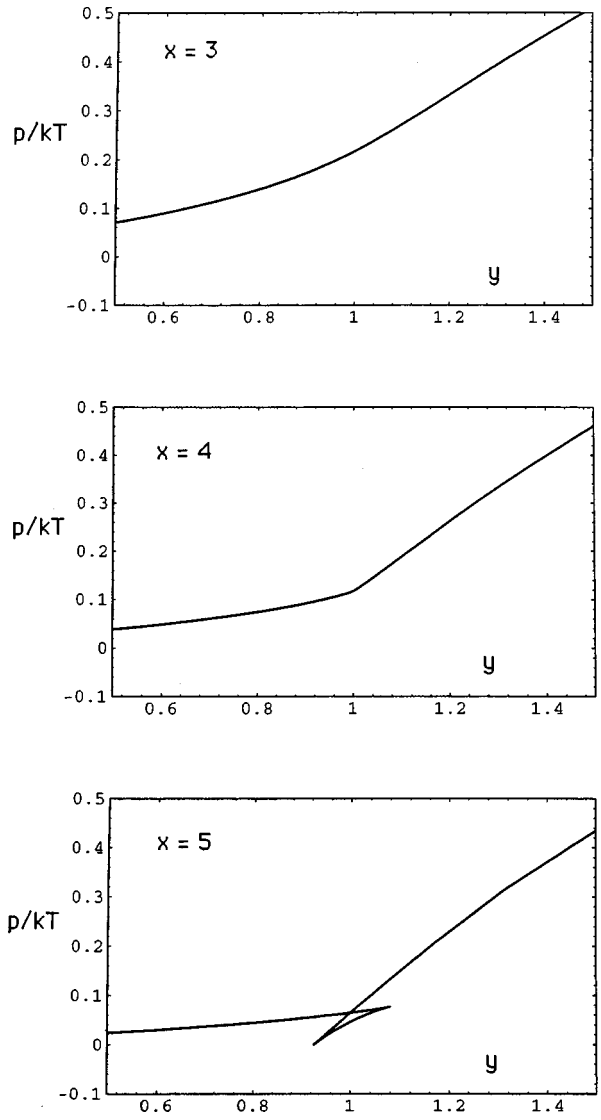

FIG. 6. The pressure p/kT as a function of fugacity for the same systems as illustrated in Fig. 5. For the case of $x>x_c$ ($T<T_c$) the function develops the swallowtail cusp that is the signature of a first-order phase transition.

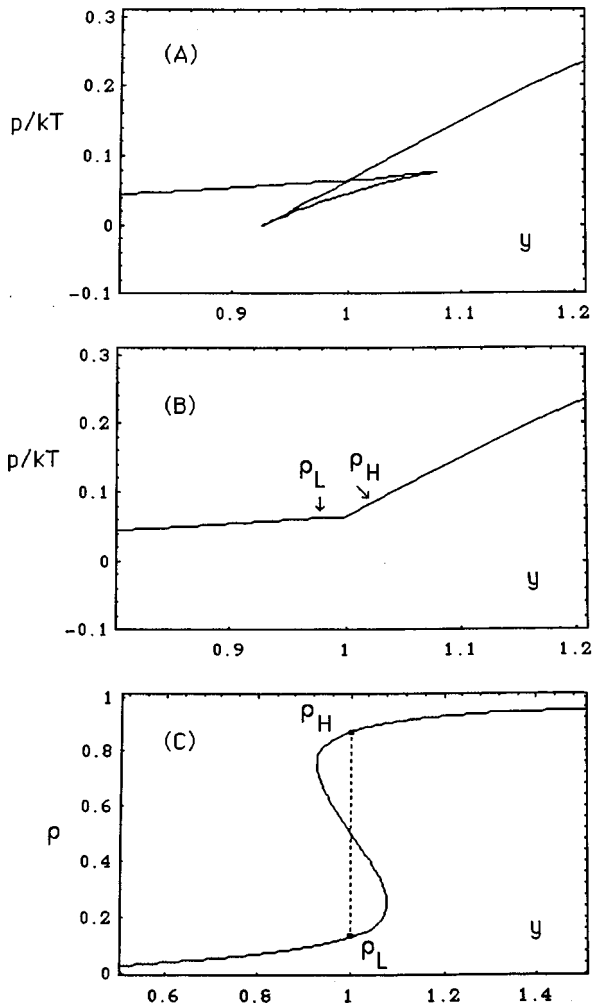

FIG. 7. A comparison of the curves from Figs. 5 and 6 for the case of $x=5>x_c$. (a) The pressure curve shown in Fig. 6. (b) The same curve as in (a) with the nonphysical swallowtail cusp removed. The symbols ρ_L and ρ_H indicate gas (low) and liquid (high) densities, respectively, that are determined by the slope of the pressure curve on either side of the phase transition singularity. (c) Interpretation of the curve shown in Fig. 5 adding a vertical discontinuity between ρ_L and ρ_H determined as indicated in (b).

$$Q=\frac{M!}{(M-N)!N!}(x^{c/2})^{\theta}, \tag{3.15}$$

where $\theta=N/M$ which is the same as the density ρ. The activity and the pressure are obtained using Eq. (2.4),

$$\beta p=-\ln(1-\rho)-(c/2)\rho^2\ln x, \tag{3.16}$$

$$\ln z=\ln[\rho/(1-\rho)]-c\rho\ln x. \tag{3.17}$$

Now instead of using Q we write an average grand partition function per site as follows:

$$\xi=1+zx^{c\theta}. \tag{3.18}$$

Then the probability a site is occupied (the density ρ) is

$$\rho=\frac{zx^{c\theta}}{1+zx^{c\theta}}. \tag{3.19}$$

But $\rho=\theta$ and solving Eq. (3.19) for z we obtain Eq. (3.17). However, if we interpret ξ of Eq. (3.18) as a proper grand partition function and take the appropriate derivative to obtain the pressure we get $\beta p=\ln\xi=\ln[\rho/(1-\rho)]$, which is incorrect. We can obtain the correct pressure by using z of Eq. (3.17) and the standard thermodynamic relation

$$\beta p=\int \rho\frac{\partial\ln z}{\partial\rho}d\rho. \tag{3.20}$$

The ξ of Eq. (3.18) is a strange construction for several reasons. First, it contains x^c while we would expect $x^{c/2}$, as in Eq. (3.15), since every bond is shared by two particles. Second, it explicitly contains the density rather than the activity. And third, it does not give the proper pressure directly.

IV. LATTICE GAS WITH EXCLUSION AND ATTRACTION

Our main purpose in this section is to treat the lattice gas on the plane-square lattice with nearest-neighbor exclusion

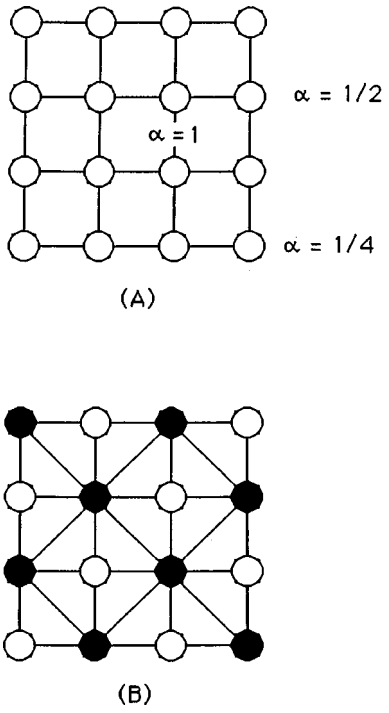

FIG. 8. Illustration of large blocks for the plane-square lattice. (a) A large square block for treating the nearest-neighbor Ising model. The values of α are shown for typical sites and indicate the nature of the factor ζ^{α} to be assigned to each type of site when occupied by a particle. The values of α are determined by how many neighboring blocks would share a site and are $\alpha=1$ (interior site, no sharing); $\alpha=\frac{1}{2}$ (side site, share with one other block); and $\alpha=\frac{1}{4}$ (corner site, share with four other blocks). (b) Maximum density of particles in the block shown in (a) with nearest-neighbor exclusion; the diagonal lines indicate next-nearest-neighbor bonds.

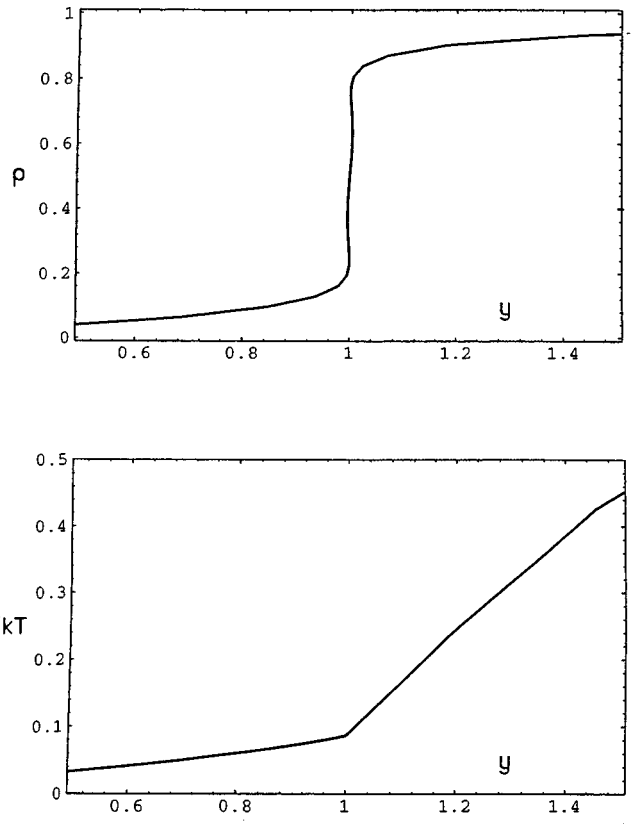

FIG. 9. The nearest-neighbor Ising model treated with the large block of Fig. 8(a). (a) The density as a function of fugacity. (b) The pressure as a function of fugacity. Both curves are evaluated at the critical value of x ($x_c=4.2048$) for the approximation shown.

and next-nearest-neighbor attraction using the generalized Bethe approximation. Before turning to that model it is useful first to briefly consider how fast the properties of the Ising model in two-dimensions converge to the exact results when the block size is increased. Using the blocks (b), (d), and (f) shown in Fig. 3 for the plane-square Ising model the critical values of x are $x_c=3.171$, 4.000, and 4.205, respectively (compared to the exact value $x_c=5.823$). We have already noted that $x_c=4$ for the simplest type of block [block (a) in Fig. 3]. Thus in going from block (a) to block (b) the estimate of the critical point gets worse [block (a) gives the exact solution for a Bethe lattice]. If one plots $u_c=1/x_c$ versus $1/n$ (labeling the blocks (b), (d), and (f) as $n=1,2,3$) one gets a smooth curve pointed toward the exact value of $u_c=0.1716$, but the rate of convergence to the exact result is very slow. Indeed, the main value of the Bethe approximation is not in calculating accurate critical parameters, but as a simple means of obtaining qualitatively correct phase diagrams for complex systems.

In Fig. 8(a) we reproduce block (f) and indicate representative values of the exponent α required to construct the block grand partition function ξ. Recall that α measures the extent to which a particle at a particular site in a block is shared with neighboring blocks. Thus an interior site that is not shared at all has $\alpha=1$, an edge site that is shared between two blocks has $\alpha=\frac{1}{2}$ and a corner site that is shared between four blocks has $\alpha=\frac{1}{4}$. The correct assignment of the α's through the ζ^{α} factors in the construction of ξ is the crucial part of the generalized Bethe approximation. For the large square indicated in Fig. 8(a) the critical value of x (marking the value of x at which one first obtains the swallowtail cusp illustrated in Fig. 7) is $x_c=4.025$. In Fig. 9 we illustrate the variation of the density and the pressure as function of fugacity for block (f) at $x=x_c$. For the large square one sees that the density curve is very sharp indeed, reflecting the very flat nature of the coexistence curve for the Ising model in two dimensions.

The lattice gas model on the plane-square lattice with nearest-neighbor exclusion has been studied by many authors as a prototype model for the gas-solid phase transition (in contrast to the gas-liquid phase transition exhibited by the standard Ising model). Early treatments were given by Gaunt and Fisher [13], Runnels and Combs [14], and Ree and Chestnut [15] while more recent investigations have been given by Poland [16], Baram and Fixman [17], and Todo and Suzuki [18].

The central feature of the model is that at high density the particles must sit on alternating lattice sites due to the requirement of nearest-neighbor exclusion. Since there are two sets of alternating sites (two sublattices), the system must pick one of them (sublattice ordering). It is found that there is a second-order phase transition in the system that marks the onset of sublattice order. Only one lattice gas model with excluded volume has been solved exactly and that is the hard-hexagon model of Baxter [19]. That model has a

second-order phase transition at a critical value of the activity given by $z_c = 11.09$. For the model with nearest-neighbor exclusion on the plane-square lattice, the value of the activity at which this transition occurs is known [18] with very high accuracy (uncertainty in the last digit)

$$\ln z_c = 1.334\,015\,10(1) \tag{4.1}$$

or (rounding off)

$$z_c = 3.796\,255. \tag{4.2}$$

The critical value of the density is [13–15]

$$\rho_c = 0.3678(1). \tag{4.3}$$

We now apply the generalized Bethe approximation to the above model with the added feature of next-nearest-neighbor attractions. The phase diagram of this model has been obtained using exact series expansion [20], so we have a comparison for the results obtained from the Bethe approximation. We have previously compared the results obtained from exact series with those obtained from the Bethe approximation for another system [21].

For the generalized Bethe approximation we require the pressure and the activity as a function of density in the high-temperature limit, i.e., the model with nearest-neighbor exclusion described above. Thus our reference system in the generalized Bethe approximation already has a critical point (second-order phase transition marking the onset of sublattice order). Both low- and high-density activity series are known for this high-temperature limit as a by-product of series for the Ising model [13]. Baxter, Enting and Tsang [22] have given 42 terms in the low-density series and 24 terms in the high-density series. We will use a modest number of these terms (15 terms in the low-density series, nine terms in the high-density series) to construct Padé approximants for the required functions from both the low-and high-density sides. We convert the activity series to density series and then use a $(\frac{7}{8})$ Padé approximant to fit the low-density functions and a $(\frac{4}{5})$ Padé approximant to fit the high-density functions. For $\rho < \rho_c$ we use the low-density branches, while for $\rho > \rho_c$ we use the high-density branches [ρ_c given in Eq. (4.3)]. The Padé approximants do not quite match at ρ_c so we add a correction (tenth order in the density) to the high-density functions so that there is no discontinuity where the branches join. The functions $z(\rho)$ and $p(\rho)/kT$ obtained in this manner are shown in Fig. 10 where the solid dots mark the position of the critical point. One sees that the second-order phase transition in the hardcore system involves only a subtle inflection in the curves at ρ_c.

We now add in next-nearest-neighbor attractions. These interactions are illustrated by the diagonal lines in Fig. 8(b) which shows the close-packing limit for the block shown in Fig. 8(a). Nearest-neighbor exclusion forces the particles to sit on alternate sites and the next-nearest-neighbor attractions reinforce that structure. Thus the two types of interaction both favor sublattice order. From our study of this model using exact series [20] we found that the second-order transition persists as the temperature is lowered from infinity down to a tricritical temperature below which the transition becomes first order. The tricritical point is where the gas and

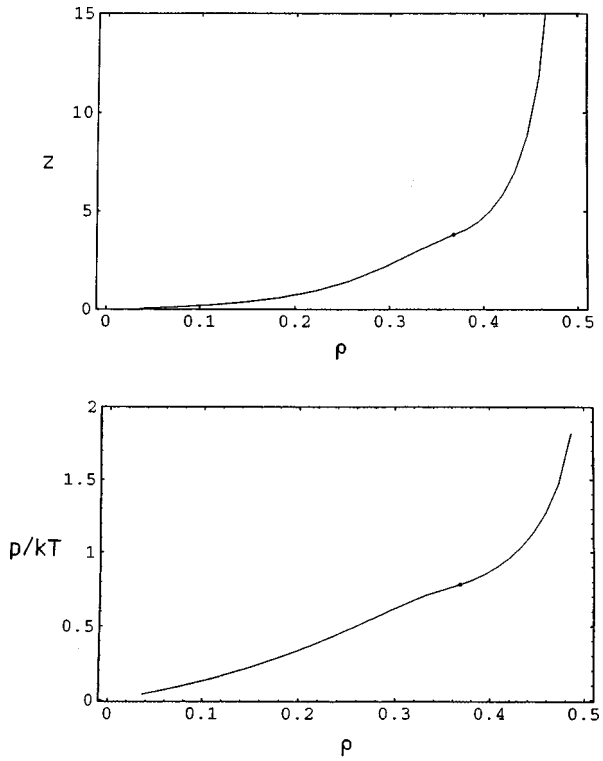

FIG. 10. The high-temperature limit for the model with nearest-neighbor exclusion and next-nearest-neighbor attraction. The curves show Padé approximants based on exact low- and high-density activity series. (a) The pressure as a function of fugacity. (b) The density as a function of fugacity. The solid dot in each curve indicates the second-order phase transition marking the onset of sublattice order.

the two sublattice phases are all in equilibrium. We estimated the following tricritical parameters:

$$x_{\mathrm{tcp}} = 3.65 \quad \text{and} \quad \rho_{\mathrm{tcp}} = 0.29. \tag{4.4}$$

We also obtained exact low-temperature expansions of the fugacity and density (low and high) along the gas-solid coexistence curve. The appropriate low-temperature parameter is

$$u = 1/x, \tag{4.5}$$

where $x = \exp[-\varepsilon/kT]$ is the Boltzmann factor for the next-nearest-neighbor interaction.

To apply the generalized Bethe approximation to this model we require, in addition to the high-temperature limits for the activity and the pressure shown in Fig. 10, the grand partition function ξ for the block of lattice sites shown in Fig. 8(b). Since there are 16 lattice sites in the block, ξ is a sum over 2^{16} different particle configurations (many of these are forbidden due to nearest-neighbor exclusion). All of the terms in ξ are products of the Boltzmann factor x for the attractive interactions and the block activity ζ. The exponents for the site factors ζ^{α} are illustrated in Fig. 8(a) (where we have $\alpha = \frac{1}{4}$, $\frac{1}{2}$, and 1, respectively, for corner, edge, and interior sites). We have chosen the block shown in Fig. 8(b) for this model specifically because there are no interactions between particles in the interior of one block with those in the

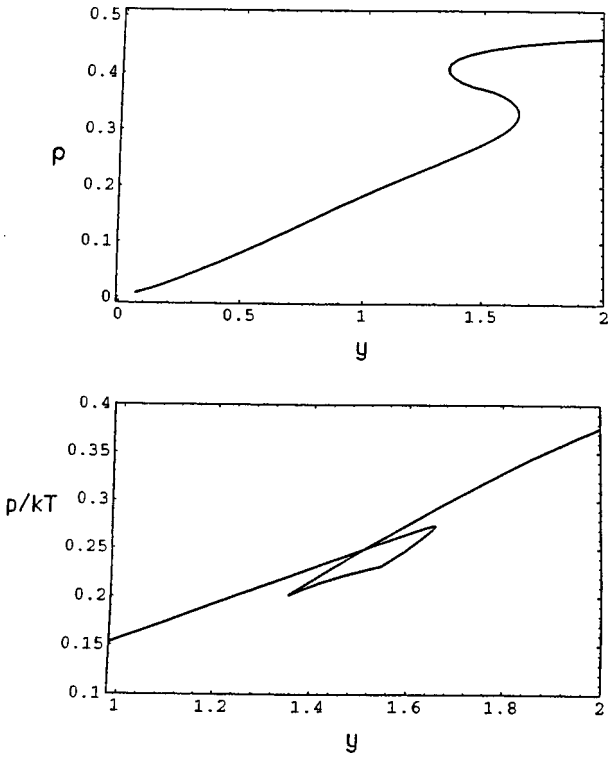

FIG. 11. The lattice gas with nearest-neighbor exclusion and next-nearest-neighbor attraction treated with the large block of Fig. 8(b). (a) The density as a function of fugacity. (b) The pressure as a function of fugacity. Both curves are evaluated at the critical value of $x=3$. There is a swallowtail cusp, indicating a first-order phase transition, for all $x>1$. At all temperatures there is only one phase transition.

interior of a neighboring block (a feature discussed previously in connection with Fig. 4).

We show typical behavior of the density and pressure as a function of fugacity ($y=zx^2$) in Fig. 11 for the case of $x=3$. The density curve shows van der Waals loops while the pressure curve has a swallowtail cusp, indicating a first-order phase transition (as described in Fig. 7). We find that the first-order phase transition vanishes only as $x\rightarrow 1$. Thus in the Bethe approximation the tricritical temperature is infinite. In Fig. 12 we show the density and fugacity phase diagrams showing the locus of the phase transition singularities as a function of the low-temperature parameter u defined in Eq. (4.5). The phase diagrams given in Fig. 12 are qualitatively similar to those obtained from exact series [20], except that in the Bethe approximation the transition is first order up to $x=1$. In particular, the behavior of $y_\sigma(u)$, the locus of the fugacity singularities, given by the generalized Bethe approximation is quite accurate. The main feature of the model obtained from both the Bethe approximation and by exact series is that at all temperatures there is one transition from gas to solid.

In the following paper [8] we will treat a model similar to the one just presented but with the added feature of having two types of attractive interaction, one of which does not reinforce the sublattice structure favored by nearest-neighbor exclusion. Both the generalized Bethe approximation and exact series indicate that the model exhibits a typical gas-liquid-solid phase diagram.

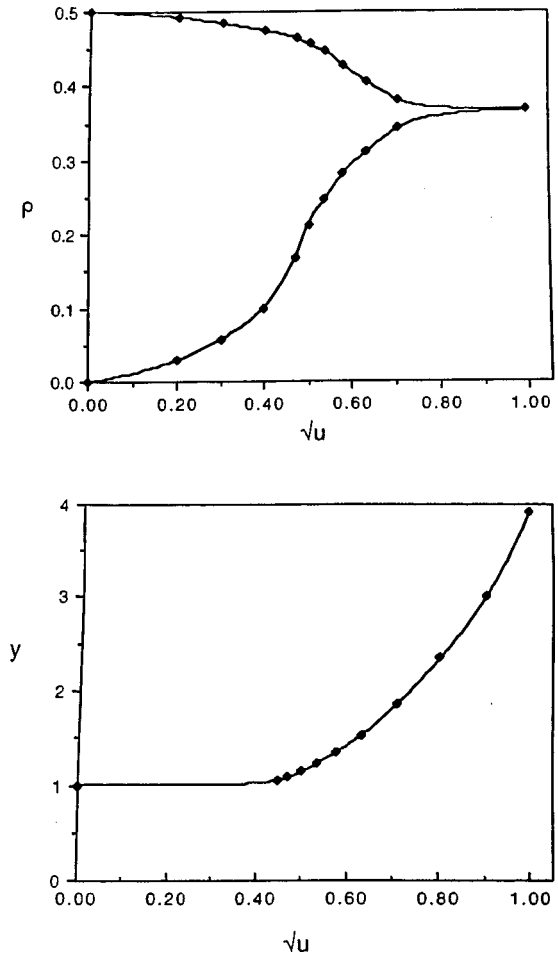

FIG. 12. The phase diagram for the lattice gas with nearest-neighbor exclusion and next-nearest-neighbor attraction treated with the large block of Fig. 8(b). The upper graph shows the coexistence curve giving the low- and high-density sides of the first-order phase transition as a function of the low-temperature parameter $u=1/x$. The lower graph shows the phase-transition value of the fugacity as a function of u.

APPENDIX

In this appendix we show that Eq. (1.1) is a property of branching Markov chains. We begin by considering the particle configurations (I) and (II) for the square-planar lattice shown in Fig. 13. They show a central lattice site surrounded by its four nearest neighbors. In (I) all of the sites are empty while in (II) the central site is filled. The probabilities of

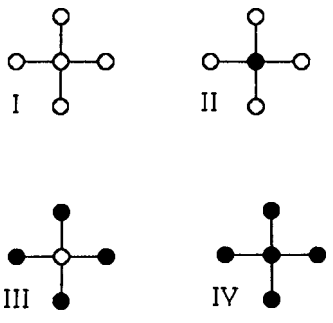

FIG. 13. Lattice configurations for the treatment of branching Markov chains.

these two structures can be written as

$$P_{\mathrm{I}}=\Xi'(1/\Xi) \quad \text{and} \quad P_{\mathrm{II}}=\Xi'(z/\Xi), \tag{A1}$$

where Ξ is the total grand partition function of the system and Ξ' is the grand partition function for all of the other particles outside of the central quintet of sites. Since interactions in this model are strictly nearest-neighbor, Ξ' is the same for (I) and (II). Thus the ratio of the probabilities is exactly

$$P_{\mathrm{II}}/P_{\mathrm{I}}=z. \tag{A2}$$

Now the central property of a branching Markov chain is that the probabilities of structures like (I) and (II) can be written in the form

$$P_{\mathrm{I}}=p_0P(0|0)^4 \quad \text{and} \quad P_{\mathrm{II}}=P_1P(1|0)^4, \tag{A3}$$

where p_0 and p_1 and the *a priori* probabilities that any site is empty or occupied, respectively, and $P(i|j)$ is the conditional probability that given state *i*, state *j* follows. Using the definition of conditional probability (where p_{ij} is the probability of finding the nearest-neighbor sequence i-j) one has

$$p_{ij}=p_iP(i|j) \quad \text{or} \quad P(i|j)=p_{ij}/pi. \tag{A4}$$

Putting all of this together gives (taking $p_1=\rho$ and $p_0=1-\rho$) for general coordination number *c*,

$$P_{\mathrm{II}}/P_{\mathrm{I}}=\left(\frac{p_{01}}{p_{00}}\right)^c\left(\frac{1-\rho}{\rho}\right)^{c-1}=z. \tag{A5}$$

We now turn to the grand partition function for a pair of sites in the Bethe approximation. For all Ising models we have

$$\xi=1+2\zeta^{1/c}+x\zeta^{2/c}. \tag{A6}$$

In this formulation, the probabilities of the various types of bonds are

$$p_{00}=1/\xi, \quad p_{10}=p_{01}=\zeta^{1/c}/\xi, \quad p_{11}=x\zeta^{2/c}/\xi. \tag{A7}$$

Using the above probabilities in Eq. (A5) gives

$$\left(\frac{1-\rho}{\rho}\right)^{c-1}\zeta(x)=z(x) \tag{A8}$$

with a similar equation for the high-temperature limit

$$\left(\frac{1-\rho}{\rho}\right)^{c-1}\zeta(1)=z(1). \tag{A9}$$

The ratio of these two equations gives

$$z(x)/z(1)=\zeta(x)/\zeta(1), \tag{A10}$$

which is our ratio formula of Eq. (1.1).

We note in passing that one of course does not need the Bethe approximation of Eq. (A6) to proceed from Eq. (A5) to a final answer. One need only consider the case of the lattice quintets (III) and (IV) shown in Fig. 13. Proceeding in the same manner as before, the ratio of the probabilities of these two structures is (we give the result for general coordination number *c*)

$$P_{\mathrm{IV}}/P_{\mathrm{III}}=zx^c\left(\frac{p_{11}}{p_{01}}\right)^c\left(\frac{p_0}{p_1}\right)^{c-1}. \tag{A11}$$

Then we use the constraints

$$p_{01}+p_{00}=p_0, \quad p_{11}+p_{10}=p_1, \quad p_{10}=p_{01}, \tag{A12}$$

which gives (again using $p_1=\rho$ and $p_0=1-\rho$)

$$p_{00}=1-\rho-p_{01}, \quad p_{11}=\rho-p_{01}. \tag{A13}$$

Taking the ratio of Eq. (A11) to (A5) gives

$$x=(\rho-p_{01})(1-\rho-p_{01})/p_{01}^2, \tag{A14}$$

which can be solved for p_{01} in terms of given values of x and ρ (it is quadratic in p_{01} independent of c). Then one can use the result of Eq. (A14) in either Eq. (A5) or (A11) to give z as an explicit function of x and ρ,

$$z=\left(\frac{1-\rho}{\rho}\right)^{c-1}\left(\frac{1}{f(x,\rho)-1}\right)^c, \tag{A15}$$

where

$$f(x,\rho)=\frac{2(x-1)(1-\rho)}{\sqrt{1+4\rho(1-\rho)(x-1)}-1}. \tag{A16}$$

This is straightforward, but the use of Eq. (A6) directly is much simpler. Referring to equations in the text, Eq. (3.11), using ζ from Eq. (3.10), gives exactly the same $z(x,\rho)$ as does Eq. (A15).

[1] H. A. Bethe, Proc. R. Soc. London, Ser. A **150**, 552 (1935).

[2] E. A. Guggenheim, *Mixtures* (Oxford, London, 1952).

[3] T. L. Hill, *An Introduction to Statistical Thermodynamics* (Dover, New York, 1986), Chap. 14, p. 252.

[4] T. L. Hill, *Statistical Thermodynamics* (Dover, New York, 1987), Chap. 7.

[5] M. E. Fisher and J. W. Essam, J. Math. Phys. **2**, 609 (1961).

[6] H. N. V. Temperley, Proc. Cambridge Philos. Soc. **40**, 239 (1944).

[7] G. S. Rushbrooke and H. D. Ursell, Proc. Cambridge Philos. Soc. **44**, 263 (1948).

[8] D. Poland, Phys. Rev. E **59**, 1523 (1999).

[9] E. A. Guggenheim, Proc. R. Soc. London, Ser. A **183**, 213 (1944).

[10] T. L. Hill, J. Chem. Phys. **18**, 988 (1950).

[11] See E. A. Guggenheim, *Mixtures* (Ref. [2]), p. 352.

[12] T. D. Lee and C. N. Yang, Phys. Rev. **87**, 404 (1952); **87**, 410 (1952).

[13] D. S. Gaunt and M. E. Fisher, J. Chem. Phys. **43**, 2840 (1965).
[14] L. K. Runnels and L. L. Combs, J. Chem. Phys. **45**, 2482 (1966).
[15] F. H. Ree and D. A. Chestnut, J. Chem. Phys. **45**, 3983 (1966).
[16] D. Poland, J. Stat. Phys. **77**, 783–806 (1994).
[17] A. Baram and M. Fixman, J. Chem. Phys. **101**, 3172 (1994).
[18] S. Todo and M. Suzuki, Int. J. Mod. Phys. C **7**, 811 (1996).
[19] R. J. Baxter, J. Phys. A **13**, L61 (1980).
[20] M. W. Springgate and D. Poland, Phys. Rev. A **20**, 1267 (1979).
[21] D. Poland, J. Chem. Phys. **71**, 1942 (1979).
[22] R. J. Baxter, I. G. Enting, and S. K. Tsang, J. Stat. Phys. **22**, 465 (1980).